TRENDS IN SCIENCES 2026; 23(6): 12398
https://doi.org/10.48048/tis.2026.12398 RESEARCH ARTICLE

In vitro Antibiofilm and Anti-Quorum Sensing Effects of Bromelain against Dual-Species Biofilms of *Streptococcus mutans* and *Fusobacterium nucleatum*

Nursyamimi Nasuha Suhaimi[1,2], Nur Ayunie Zulkepli[1,2,*], Fatimah Salim[1], Norehan Mokhtar[3], Dyaningtyas Dewi Pamungkas Putri[4] and Mohd Khairul Ya'Kub[5]

[1]*Atta-Ur-Rahman Institute for Natural Product Discovery (AuRIns), Universiti Teknologi MARA (UiTM), Selangor Branch, Puncak Alam Campus, Selangor 42300, Malaysia*
[2]*Centre for Medical Laboratory Technology Studies, Faculty of Health Sciences, Universiti Teknologi MARA (UiTM), Selangor Branch, Puncak Alam Campus, Selangor 42300, Malaysia*
[3]*Dental Simulation & Virtual Learning Research Excellence Consortium, Department of Dental Science, Advanced Medical & Dental Institute, Universiti Sains Malaysia, Pulau Pinang 13200, Malaysia*
[4]*Laboratory of Pharmacology and Toxicology, Department of Pharmacology and Clinical Pharmacy, Faculty of Pharmacy, Universitas Gadjah Mada Sekip Utara II, Yogyakarta 55281, Indonesia*
[5]*Smart KJ Agro (Asia) Plt, Bandar Amanjaya, Sungai Petani, Kedah 08000, Malaysia*

([*]Corresponding author's e-mail: nayunie@uitm.edu.my)

Received: 23 October 2025, Revised: 18 November 2025, Accepted: 25 November 2025, Published: 15 February 2026

Abstract

Periodontitis is a prevalent chronic oral disease strongly associated with biofilm formation and quorum sensing (QS) among pathogenic bacteria. Current therapeutic approaches rely on mechanical removal and antibiotics but resistance and side effects highlight the need for alternatives strategies. In this study, bromelain, a cysteine protease derived from pineapple (*Ananas comosus*) core was evaluated as a potential natural bioactive agent against biofilm-associated oral infections. Ultrafiltrated bromelain (UFB) was obtained by ammonium sulphate precipitation and ultrafiltration with SDS-PAGE confirming a bromelain protein band at 25 kDa. Antibiofilm activity was assessed using dual-species biofilms of *Streptococcus mutans* and *Fusobacterium nucleatum*. Crystal violet assays revealed concentration-dependent inhibition with biofilm biomass reduced by 23.6% at 31.25 µg/mL and up to 63.8% at 1,000 µg/mL. SEM confirmed decreased biofilm density and disrupted EPS while bacterial cell morphology remained intact suggesting matrix destabilisation rather that bactericidal effect. Furthermore, QS inhibition was evaluated using *Chromobacterium violaceum* as a biosensor. UFB significantly reduced violacein production in a concentration-dependent manner, with noticeable inhibition from 500 µg/mL (3.16%) and significant QS-inhibition of 43.23% at 1,000 µg/mL which indicated interference with QS-regulated bacterial communication and virulence. These findings demonstrated that bromelain not only disrupts biofilm formation but also impairs QS pathways, highlighting its dual role as antibiofilm and anti-QS in attenuating microbial pathogenicity. Together, this study supports the potential application of bromelain derived from pineapple core as a sustainable and natural adjunct for periodontitis management.

Keywords: Periodontitis, Oral pathogens, *Streptococcus mutans*, *Fusobacterium nucleatum*, *Chromobacterium violaceum*, Dual-species, Biofilm, Quorum sensing, Pineapple, Bromelain

Introduction

Periodontitis is a widespread chronic inflammatory disease associated with the dysbiosis of microbial communities that causes attachment and alveolar bone loss [1,2]. The pathogenesis of periodontitis is also influenced by environmental and host factors. Tobacco consumption, obesity, poor oral

hygiene, and diabetes mellitus represent modifiable risks, whereas systemic conditions, such as reduced bone mineral density and socioeconomic stressors, further predispose individuals to the disease [3,4]. According to the Global Burden of Disease (GBD) 2021, its prevalence is substantial, affecting approximately 12,500 cases per 100,000 individuals worldwide [5]. *Streptococcus mutans* is considered a key etiological agent due to its capacity to form complex three-dimensional biofilms on enamel and mucosal surfaces [6]. By acidifying the microenvironment, *S. mutans* creates favorable conditions for the colonization bridging organisms, such as *Fusobacterium nucleatum* [7,8]. The ecological disruption within the oral microbiota drives the establishment of pathogenic biofilms, which are a fundamental contributor to the onset and progression of periodontal disease.

A biofilm is a highly organized, complex three-dimensional microbial community composed of various microorganisms, primarily bacteria, embedded within a self-produced extracellular polymeric substance (EPS) [9,10]. The establishment of biofilms begins when bacterial cells adhere to surfaces through the coordinated action of motility structures and surface adhesins [11]. Microcolonies are formed and quorum sensing (QS) mechanisms are activated as the bacterial population increases. The biofilm matures over time, exhibiting organized spatial structure and metabolic cooperation among the bacterial cells [12]. Biofilm integrity is largely maintained by the EPS matrix, which serves as a structural support and a protective barrier [13,14]. This formation significantly enhances bacterial survival and promotes immune evasion, contributing to the emergence of chronic and recurrent infections [9]. QS further regulates these processes, by coordinating virulence, biofilm maturation, and resistance mechanisms.

QS is a population-dependent communication mechanism that plays a crucial role in the coordination of various physiological processes [15,16]. These behaviors are typically ineffective at the single-cell level but become advantageous when performed in synchrony by a dense bacterial community [17]. Therefore, this mechanism is vital for coordinating group behaviors that enhance bacterial survival and adaptability in diverse environments. Consequently, QS-regulated biofilms demonstrate resistance levels that can range from 10- to 1,000-fold greater than those of planktonic cells, accounting for more than 70% of bacterial infections [18]. QS enables bacteria to respond to environmental stress by modulating the expression of genes associated with stress adaptation and resistance mechanisms [19,20]. This regulation facilitates the development of resistant phenotypes within the biofilm, allowing bacteria to survive in the presence of antibiotics, oxidative stress, and immune responses. Therefore, after initial therapy, biofilm-associated infections are often persistent, difficult to treat, and prone to recurrence [9]. The presence of a weakened immune system further accelerates the spread and severity of these biofilm-related diseases. Furthermore, the QS-controlled regulation of biofilm formation and toxin production underscores its importance as a target for novel antimicrobial strategies aimed at disrupting bacterial communication and pathogenicity.

Therefore, targeting QS and biofilm matrices with enzyme-based strategies is an attractive adjunct to conventional antimicrobials. Bromelain, a cysteine protease derived from pineapple (*Ananas comosus*), is a naturally occurring enzyme with proteolytic activity and low toxicity [21,22]. It interferes with microbial adhesion and matrix integrity and exhibits diverse biological functions, including anti-inflammatory [23], antibacterial [24], antibiofilm [25], antioxidant [26], anti-cancer [27], and anticoagulant [28] activities. Although some studies suggest that bromelain may influence QS by disrupting signaling molecules and limiting microbial communication, there is a scarcity of evidence. Therefore, its potential to inhibit dual-species oral biofilms and QS remains largely underexplored.

Materials and methods

Bacterial strains

Stock cultures of *S. mutans* (ATCC 25175), *F. nucleatum* (ATCC 10953), and *C. violaceum* (ATCC 12672) were purchased from the American Type Culture Collection (ATCC) in freeze-dried form. The selected bacteria were cultured in Brain Heart Infusion (BHI) broth and Luria Bertani (LB) broth at 37 °C under suitable atmospheric conditions. Gram staining was performed to confirm the identity and purity of the bacterial inoculum.

Preparation of Ultrafiltrated Bromelain (UFB)

The extraction of bromelain from the Millie Dillard-2 (MD2) hybrid pineapple core was performed in accordance with the protocol comprising crude extraction, ammonium sulfate precipitation, and ultrafiltration [29]. The pineapple core was blended with distilled water and centrifuged at 6,000 rpm for 40 min at 4 °C. The supernatant was treated with 0.01% pectinase, followed by protein precipitation using 50 %(w/v) ammonium sulfate at 4 °C overnight. The resulting pellet was dissolved in 0.2 M phosphate buffer (pH 7) in an equal volume after a second centrifugation. The solution was then filtered through a 0.22 µm membrane and concentrated via ultrafiltration at 6,000 rpm for 30 min using Amicon ultrafiltration tubes to yield the final UFB. The UFB was then quantified using NanoDrop™ 2000/2000c Spectrophotometers (Thermo Scientific) for validation.

Visualization of bromelain enzyme

Sodium dodecyl sulfate polyacrylamide gel electrophoresis (SDS-PAGE) was conducted to determine the molecular weight of UFB [30]. A commercially available bromelain standard (10,000 µg/mL; molecular weight 23 - 25 kDa) served as the reference control, while different UFB concentrations (31.25, 62.5, 125, 250, 500 and 1,000 µg/mL) were used for visualization. The UFB was mixed with the sample buffer and denatured by heating at 95 °C for 5 min. Electrophoresis was performed at a constant voltage of 100 V using a gel composed of 4% stacking and 12% resolving layers. The bromelain standard and a protein molecular weight marker were loaded into the gel along with UFB. The gel was electrophoretically stained with Coomassie Brilliant Blue for 15 min and destained overnight in 10% acetic acid. Protein bands were visualized and captured using a gel documentation system (ImageQuant™ LAS 500).

Development and validation of a Dual-species biofilm model

The dual-species biofilm model was established using *S. mutans* and *F. nucleatum* with several modifications [31]. Prior to inoculation, the cultures of *S. mutans* and *F. nucleatum* were standardized to 0.5 McFarland standard using BHI broth at a ratio of 1:1. To develop the dual-species biofilm 1,250 µL of each standardized bacterial suspension was added to a 6-well plate containing a sterile glass coverslip, supplemented with 2% sucrose and fructose as a nutrient source. The plate was then anaerobically incubated at 37 °C for 5 days using a GasPak Anaerobic Jar system. The formed biofilms on the coverslips were washed with sterile phosphate-buffered saline (PBS) to remove any unbound bacteria. The coverslips were stained with 2% crystal violet and observed under a light microscope. Subsequent biofilm validation was performed by visualizing biofilm formation under a scanning electron microscope (SEM) to confirm the presence of both *S. mutans* and *F. nucleatum* in the sample.

Crystal violet inhibition assay

The antibiofilm activity of UFB against dual-species biofilms was evaluated using a crystal violet assay [32]. The dual-species biofilm was first developed in a 96-well plate as described above. After the initial incubation period, various UFB concentrations (0, 31.25, 62.5, 125, 250, 500 and 1000 µg/mL) were introduced into each well. The negative control (untreated dual-species biofilm) was included for reference in the calculation of biofilm inhibition percentage. Then, the plate was incubated for an additional 18 h at 37 °C under appropriate atmospheric conditions. The supernatant was carefully removed after incubation, and the wells were gently rinsed with 200 µL PBS to remove non-adherent cells. The plates were then air-dried at room temperature for 2 h. Subsequently, 200 µL of 0.1 %(v/v) crystal violet was added to each well and plate was incubated for 15 min. To quantify the biofilm biomass, 96% ethanol was added to solubilize the crystal violet, and the absorbance was measured at 590 nm using a microplate reader (SPECTROstar® Nano, BMG Labtech). This assay was performed in triplicate and repeated in three independent experiments. The percentage of UFB biofilm inhibition was calculated using the following formula:

$$Biofilm\ inhibition: \frac{Untreated\ control\ 590\ nm - Treated\ sample\ 590\ nm}{Untreated\ control\ 590\ nm} \times 100\ \% \quad (1)$$

Scanning Electron Microscope (SEM) analysis

The biofilm morphology following UFB treatment was visualized using SEM [33]. Dual-species biofilms

were prepared on 13-mm glass coverslips in 6-well plates as previously described. Biofilms were fixed with 2.5% glutaraldehyde at 4 °C for 4 - 6 h and washed three times with 0.1 M sodium cacodylate buffer at room temperature. Post-fixation was performed in 1% osmium tetroxide for 2 h at 4 °C, followed by three additional buffer washes. A graded ethanol dehydration series (35%, 50%, 75% and 95% for 10 min each) was used, followed by three 15-min immersions in 100% ethanol. The samples were allowed to dry overnight. Dried coverslips were mounted onto aluminum SEM stubs and coated with a thin layer of platinum. SEM imaging was performed at 2,500× magnification, followed by higher magnifications (5,000×, 10,000× and 20,000×). Structural differences between UFB-treated and control biofilms, such as bacterial shape alterations and EPS matrix reduction, were analyzed.

Violacein inhibition assay

The violacein inhibition assay was conducted to evaluate the QS inhibitory effect of UFB on *C. violaceum* [34]. *C. violaceum* was cultured in 10 mL of LB broth and incubated overnight at 30 °C in a shaking incubator at 2,500 rpm. The culture was then standardized to 0.5 McFarland turbidity using LB broth. Different concentrations of UFB (0, 31.25, 62.5, 125, 250, 500 and 1,000 µg/mL) were prepared in sterile tubes containing 5 mL of LB broth. Each tube was inoculated with 100 µL of the standardized *C. violaceum* suspension and incubated in a shaking incubator overnight. The negative control (without UFB) was included for reference in the calculation of violacein inhibition. After incubation, 1 mL of each culture was transferred into sterile centrifuge tubes and centrifuged at 2,500 rpm for 10 min. The pellet was dissolved in 1 mL of dimethyl sulfoxide and vortexed until completely solubilized. A second centrifugation was performed under the same conditions. Then 200 µL of resulting supernatant, were transferred into 96-well plates, and the absorbance was measured at 595 nm using a microplate reader (SPECTROstar® Nano, BMG Labtech). The assay was performed in triplicate and repeated in three independent experiments. The percentage of violacein production inhibition was calculated using the formula below:

$$Violacein\ inhibition: \frac{Untreated\ control\ 595\ nm - Treated\ sample\ 595\ nm}{Untreated\ control\ 595\ nm} \times 100\ \% \quad (2)$$

Statistical analysis

A one-way analysis of variance (ANOVA) was employed to assess the significance of UFB treatment on biofilm inhibition and violacein production. Analyses were conducted at a 95% confidence interval with a significance threshold of $p < 0.0001$. The results were analyzed using GraphPad Prism version 10.5.

Results and discussion

Periodontitis is a biofilm-mediated oral disease characterized by the demineralization of tooth structures, and affects individuals across all age groups [35]. *F. nucleatum* acts as a bridging species, facilitating the co-aggregation of early and late colonizers within subgingival biofilms, while *S. mutans*, traditionally linked to dental caries, also contributes to biofilm development and community stability [36,37]. The interactions between these bacteria within the biofilm microenvironment enhance virulence and promote the destruction of periodontal tissue. QS regulates interspecies communication and virulence expression, thereby contributing to the persistence and pathogenicity of periodontal biofilms [38]. The global burden of periodontal disease remains high, with recent estimates indicating that over 950 million people were affected by 2021 [39]. Although sodium fluoride and chlorhexidine are widely used in conventional preventive strategies, their use is limited by undesirable side effects, including tooth discoloration, taste disturbances, and oral mucosal irritation [40]. Consequently, there has been a growing interest in exploring natural bioactive agents as safer alternatives. However, a common limitation of natural compounds is the need for relatively high concentrations to achieve antimicrobial or antibiofilm effects comparable to those of conventional antibiotics [41]. UFB exhibits significant inhibitory effects against mono-species biofilms of *S. mutans* and *S. aureus* [29], highlighting its proteolytic ability to disrupt EPS matrices and microbial adhesion. However, the interaction of dual-species biofilms, particularly *S. mutans* and *F. nucleatum*, and their QS regulatory mechanisms has not been previously characterized. Therefore, this study evaluated the potential of UFB extracted from pineapple in

modulating biofilm formation and QS activity within a dual-species oral biofilm.

Bacterial morphology

Figure 1 illustrates the morphological characteristics of the investigated bacterial species, including *S. mutans*, *F. nucleatum*, and *C. violaceum,* as observed using light microscopy. As shown in (**Figure 1(A)**), *S. mutans* exhibited the typical morphology of Gram-positive cocci, arranged predominantly in chain-like formations. In contrast, (**Figures 1(B)** and **1(C)**) depict Gram-negative bacterial cells. *F. nucleatum* was distinguished by its elongated bacillary structure and its requirement for strict anaerobic growth conditions, consistent with its classification as an obligate anaerobe. *C. violaceum* was characterized by its coccobacillary morphology, which aligns with its classification as a Gram-negative facultative anaerobe, commonly used in QS studies.

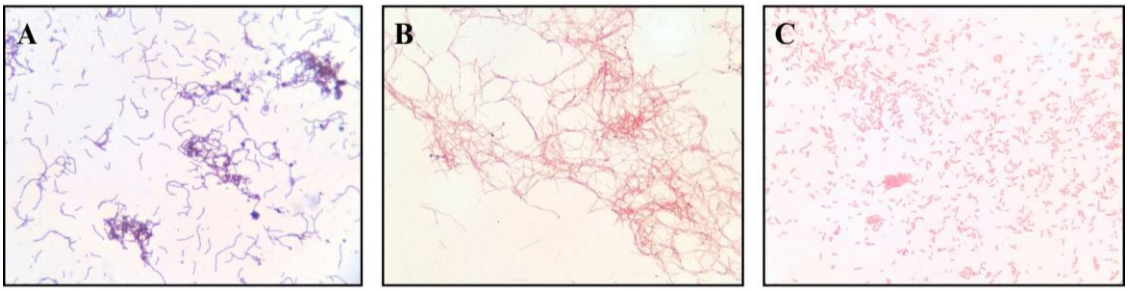

Figure 1 Gram stain results of (A) *S. mutans*, (B) *F. nucleatum*, and (C) *C. violaceum* at 100× magnification.

Protein quantification and bromelain detection

The bromelain content of the UFB sample was quantified using NanoDrop spectrophotometry at 260 - 280 nm (**Table 1**). The chromatography revealed a distinct protein peak, yielding a concentration of 4.650 mg/mL. In addition, the 260/280 ratio of 0.54 further indicated a high abundance of protein within the sample. **Figure 2** displays the protein banding patterns obtained through SDS-PAGE analysis using a 12% polyacrylamide gel, comparing a bromelain standard with various concentrations of the UFB sample. A consistent protein band at ~25 kDa was observed across all lanes, which corresponded to the expected bromelain molecular weight. The band intensity increased proportionally with UFB concentrations (31.25 - 1,000 µg/mL), reflecting dose-dependent protein levels. The absence of additional bands, suggested the high purity of the bromelain present in the UFB samples was suggested.

Table 1 Protein concentration in UFB sample by using NanoDrop spectrophotometer.

Sample	Mean of protein concentration (mg/mL)	A280 (Abs)	260/280
UFB	4.650	4.650	0.54

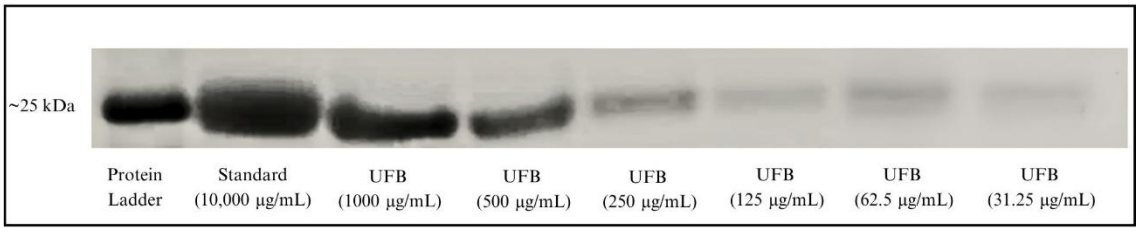

Figure 2 The detection of bromelain enzyme by using SDS-PAGE analysis.

The study started with the preparation of the UFB using the standardization method [29]. SDS-PAGE was employed to evaluate the purity of bromelain obtained from the pineapple core, demonstrating the presence of the enzyme with few impurities [42]. Therefore, the presence of bromelain enzyme in the prepared sample was confirmed by visualizing the protein of interest using 12% polyacrylamide gel. A bromelain standard with a concentration of 10,000 µg/mL was used as a reference for comparison with the targeted protein. All protein bands were consistently aligned in one line around ~ 25kDa. The expressed proteins were presumed to be the protein of interest (bromelain enzyme) with the same molecular weight as the previously reported bromelain [42]. This enzyme can be in range from 20 to 30 kDa due to several factors, such as the pineapple species, parts (pulp, peel, crown, or core), and the purification method used to obtain the enzyme content [42-45].

Establishment and microscopic visualization of a Dual-species biofilm model

Figure 3 illustrates the establishment of a dual-species biofilm model composed of the oral pathogens *S. mutans* and *F. nucleatum*, visualized by light microscopy following crystal violet staining and scanning electron microscopy. At 40× magnification, the biofilm appeared as a dense, multilayered structure covering nearly the entire microscopic field, consistent with robust surface colonization (**Figure 3(A)**). The biofilm architecture and distribution were visible, but the individual bacterial morphology could not be resolved. At higher magnification (100×), examination of a region with reduced biofilm density allowed clear visualization of distinct bacterial morphologies, corresponding to cocci and bacilli (**Figure 3(B)**). Validation by SEM at 10,000× magnification further confirmed the existence of both species, with *S. mutans* appearing predominantly as cocci intermingled with rod-shaped *F. nucleatum* embedded within the extracellular matrix (**Figure 3(C)**). These observations confirm the successful co-culture and spatial co-existence of both species, thereby validating the dual-species biofilm model for downstream experimental assays.

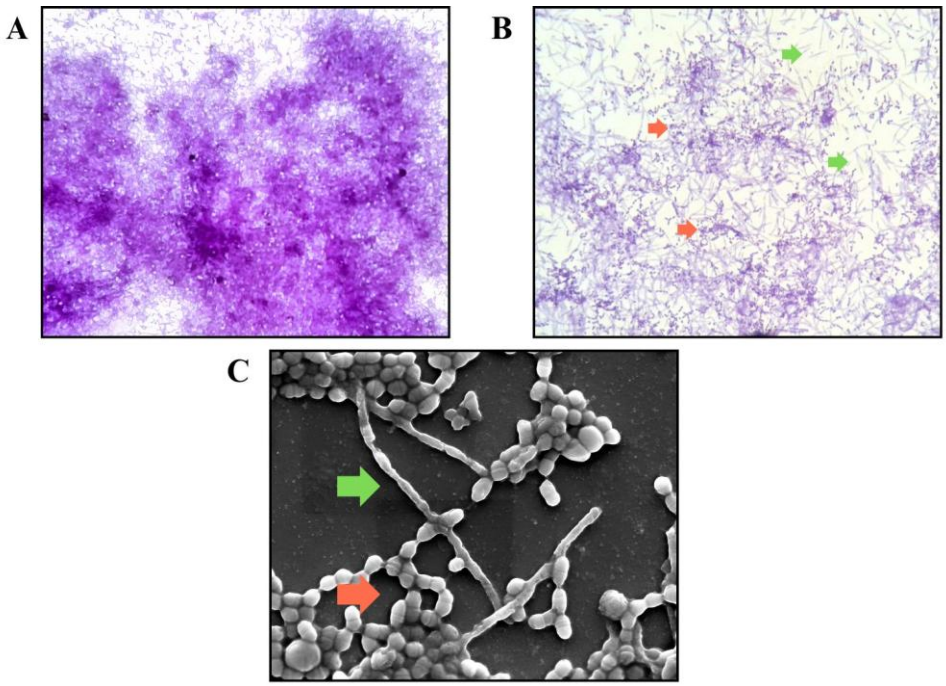

Figure 3 Dual-species biofilm formation of *S. mutans* and *F. nucleatum* was visualized using light microscope and SEM with three different magnifications. (A) 40× magnification, (B) 100× magnification, and (C) 10,000× magnification. *S. mutans* appearing as cocci (indicated by red arrows) and *F. nucleatum* as bacilli (indicated by green arrows).

Antibiofilm activity of UFB

A quantitative biofilm inhibition assay was conducted to determine the antibiofilm efficacy of UFB against preformed dual-species biofilms. As shown in **Figure 4**, UFB exhibited a concentration-dependent inhibitory effect with the biofilm biomass reduction increasing from 23.60% at 31.25 µg/mL to 63.80% at 1,000 µg/mL. At sub-inhibitory concentrations, biofilm suppression increased incrementally by approximately 10% with each two-fold increase in UFB, reaching 51.52% inhibition at 250 µg/mL. A plateau effect was observed between 250 and 500 µg/mL (52.16%), indicating a potential saturation threshold in UFB-mediated matrix disruption. The highest concentration (1,000 µg/mL) achieved the strongest inhibition, representing the maximum disruption of the biofilm structure in this study. Statistical analysis confirmed that all UFB concentrations significantly reduced the biofilm biomass compared with the untreated control ($p < 0.0001$). These findings indicate that UFB exerts potent, dose-dependent antibiofilm activity against *S. mutans*–*F. nucleatum* dual-species biofilms, primarily through the disruption of the biofilm structural integrity rather than complete eradication.

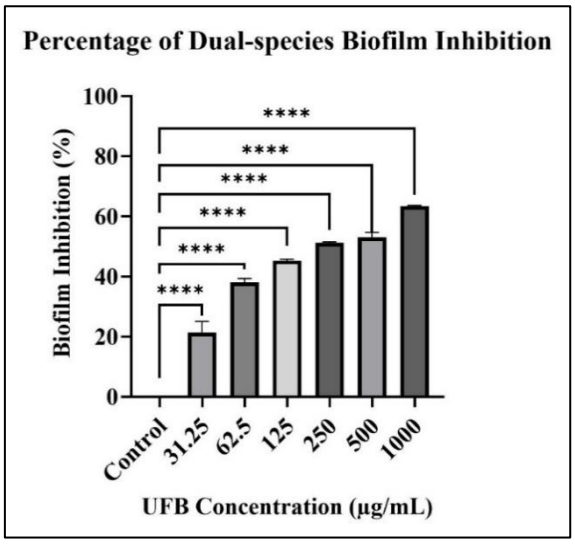

Figure 4 Percentage of biofilm inhibition of dual-species biofilm of *S. mutans* and *F. nucleatum* against different UFB concentrations. **** ($p < 0.0001$) indicate significant differences when compared to negative control.

The initial analysis to determine the inhibitory effects of UFB on dual-species biofilm was conducted using the crystal violet assay, a gold standard method. The present findings demonstrated a concentration-dependent inhibition of dual-species oral biofilms by UFB, with inhibition ranging from 23.6% - 63.8% ($p < 0.0001$). These results are consistent with those of contemporary efforts to harness natural compounds to disrupt oral biofilms. For instance, a previous study showed strong evidence of the effectiveness of Mediterranean herb extracts in combating *S. mutans* biofilms even at the lowest concentration used (150 µg/mL) [42]. This suggests that other natural extracts can achieve similar biofilm inhibition upon treatment even at the lowest concentration. Combinations of *Glycyrrhizae Radix* and *Rubi Fructus* extracts synergistically inhibit *S. mutans* biofilms by inhibiting glucosyltransferase activity, thereby impairing EPS synthesis, which is critical for biofilm integrity [41]. In addition, polyphenolic compounds derived from tea, such as epigallocatechin gallate (EGCG) from green tea and theaflavins from black tea, suppress the growth and biofilm development of *F. nucleatum* by attenuating the key virulence traits, such as hemolytic activity and hydrogen sulfide production [1]. These findings underscore the therapeutic potential of plant-derived agents acting on distinct virulence mechanisms.

Structural disruption of the biofilm architecture by UFB

The SEM analysis density and structural organization of the dual-species biofilms were compared using SEM under different conditions (**Figure 5**). SEM images at 5,000× magnification

revealed a compact, multilayered biofilm architecture consistent with a mature microbial consortium of *S. mutans* and *F. nucleatum*. In contrast, biofilms exposed to 1,000 µg/mL UFB displayed markedly reduced cell density, with microorganisms distributed sparsely and arranged predominantly in a monolayer. At higher magnification (20,000×), the EPS, which provides the structural framework and mechanical stability of the biofilms, appeared abundant and well-preserved in the control group. Conversely, the UFB-treated samples exhibited a visibly disrupted and contracted EPS matrix, indicating biofilm integrity enzymatic destabilization. The morphological characteristics of *S. mutans* (coccoid) and *F. nucleatum* (bacillary) cells remained intact after treatment, suggesting that UFB exerts its antibiofilm activity primarily through matrix degradation rather than through direct bactericidal effects.

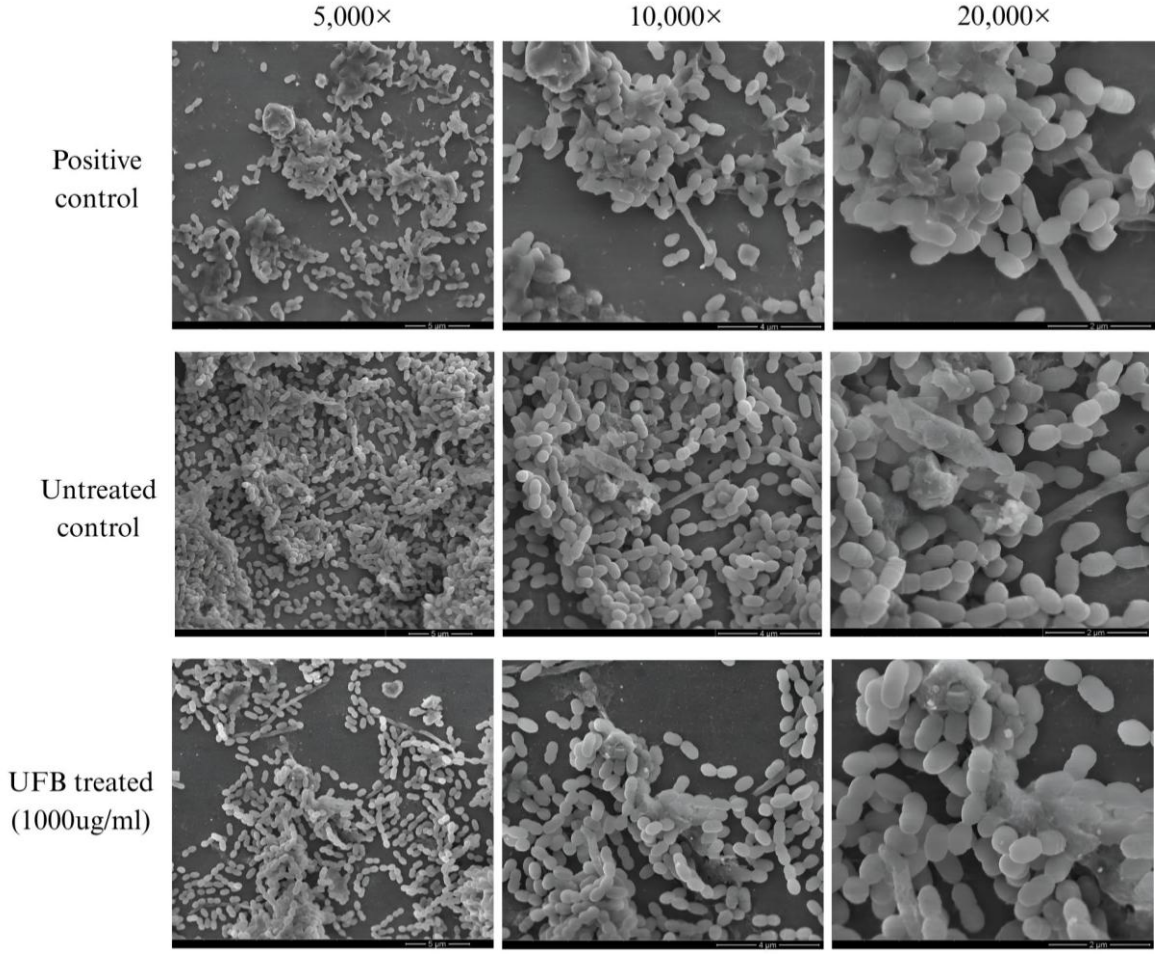

Figure 5 Visualization of dual species *S. mutans* and *F. nucleatum* biofilms at the magnification of 5,000×, 10,000× and 20,000×. SEM analysis was performed to compare the biofilm density between the controlled biofilm and UFB treated biofilm.

To validate the results of the biofilm inhibition, SEM analysis was performed. The highest inhibition concentration (63.8%) was chosen to run the analysis together with the control and the positive control. In the control group, the biofilm displayed a densely packed, multilayered organization with abundant EPS, reflecting the typical integrity of mature *S. mutans* and *F. nucleatum* biofilms. The intact EPS scaffold observed in the control highlights its essential role in maintaining biofilm cohesion and stability. In contrast, UFB treatment at 1,000 µg/mL markedly reduced the biofilm density, where it appeared more dispersed in the monolayer arrangements. Furthermore, the EPS matrix in the treated samples appeared to be disrupted and contracted, whereas the cell morphology of both species remained unchanged. These findings indicate that the

principal activity of UFB is directed toward destabilizing the biofilm matrix rather than exerting a direct bactericidal effect.

This mode of action is consistent with previous reports on natural products that interfere with biofilm integrity while preserving cell viability. For instance, anthocyanin-rich extracts from *Clitoria ternatea* demonstrated significant antibiofilm effects against oral pathogens, including *S. mutans*, where SEM imaging confirmed the disassembly of the EPS network without bacterial cell lysis [46]. Similarly, thymoquinone, a bioactive compound from *Nigella sativa*, reduced the biomass and altered the structure of *F. nucleatum*-associated biofilms, primarily by interfering with microbial adhesion and matrix stability, as revealed by SEM [47]. In addition, luteolin, a dietary flavone, has been shown to inhibit *S. mutans* biofilm development by downregulating EPS production and virulence gene expression, again without marked bactericidal effects [40]. These studies suggest that UFB shares a mode of action with other natural products, exerting potent antibiofilm activity through the disruption of matrix integrity and virulence regulation without compromising bacterial cell viability.

Anti-Quorum sensing activity of the UFB

Figure 6 depicts the effect of UFB on QS-regulated violacein production in *C. violaceum*. A two-fold concentration gradient of UFB was applied (31.25 - 1,000 µg/mL) was applied to evaluate its impact on QS-regulated pigment production. The inhibitory effect of UFB on violacein was dose-dependent, with higher concentrations resulting in reduced pigment formation (**Figure 6(A)**). At sub-inhibitory concentrations (3.125 - 250 µg/mL), violacein production remained incomparable to that of the untreated control, indicating that low doses of UFB did not interfere with QS signaling. (**Figure 6(B)**) shows a minimal reduction detected at 500 µg/mL with 3.16% inhibition, whereas a significant suppression was observed at 1,000 µg/mL (43.24%) relative to the untreated control ($p < 0.0001$). These results suggest that UFB exerts a threshold-dependent inhibitory effect on violacein production by disrupting QS regulatory mechanisms.

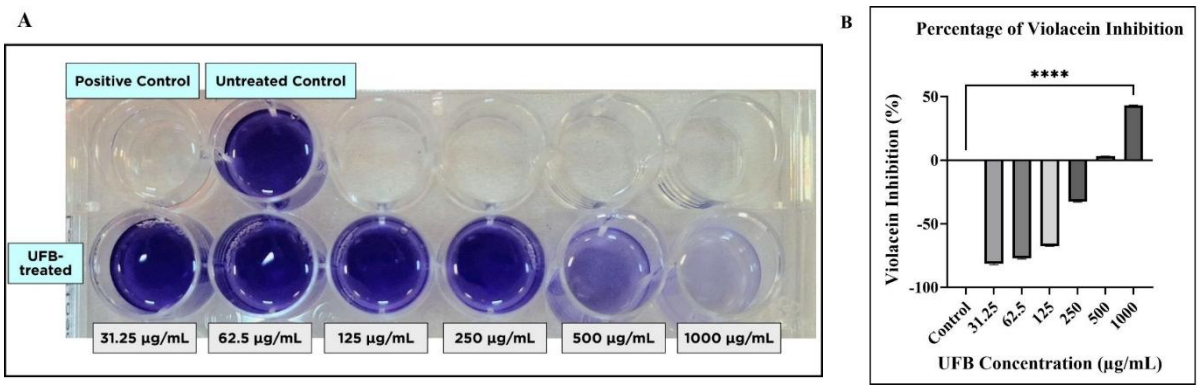

Figure 6 Violacein inhibition of *C. violaceum* at various UFB concentrations. (A) Visualization of violacein pigment upon UFB treatment, and (B) Percentage of the pigment inhibition. **** ($p < 0.0001$) indicate significant differences when compared to the control.

The ability of UFB to interfere with the integrity of dual-species biofilm suggested that its activity may be linked to QS interference. Extending this observation, we confirmed that UFB exerts a concentration-dependent inhibitory effect on violacein production in *C. violaceum*. At concentrations of 31.25 - 250 µg/mL, violacein synthesis remained unaffected, while a slight reduction (3.16%) was observed at 500 µg/mL. A marked suppression of 43.24% was observed at 1,000 µg/mL ($p < 0.0001$), indicating that UFB disrupts QS pathways only at higher concentrations. These results are consistent with those of previous reports on natural QS inhibitors, where *Passiflora edulis* extract was found to suppress violacein production in *C. violaceum* by 75.8% at sub-MIC levels [15]. Similarly, medicinal plant extracts from Iran, such as *Dionysia revoluta*, *Eucalyptus camaldulensis*, and *Syzygium aromaticum*, were reported to attenuate violacein production in *C. violaceum* in a dose-dependent manner, supporting the concept of threshold-mediated inhibition

[48]. Complementarily, a study reported that *Inula spp.* extracts inhibited violacein production in *C. violaceum* at 250 µg/mL, which was the same concentration that showed reduction by the UFB in our study [49]. The pattern of violacein inhibition observed for UFB showed notable reduction in our study. These results indicate that UFB may exert effects comparable to those of established plant-derived QS inhibitors. In addition, the extracts impaired bacterial motility and reduced biofilm development, further supporting the role of natural products in disrupting QS-regulated phenotypes.

Conclusions

Taken together, this study suggests that UFB functions analogously to other plant-derived bioactive compounds, with its antibiofilm effects largely mediated through the disruption of extracellular scaffolding and interspecies interactions. These findings reinforce the mechanistic similarities of UFB with other natural QS inhibitors, supporting its role as a candidate for controlling biofilm-associated infections. Strategies targeting biofilm density and the EPS matrix may provide advantages in controlling polymicrobial oral biofilms by weakening their structural stability and pathogenicity while minimizing the resistance commonly induced by bactericidal agents. In summary, UFB is a promising natural antibiofilm agent with dose-responsive efficacy against dual-species oral biofilms, which complements and expands upon established plant-derived strategies targeting the virulence mechanisms of *S. mutans* and *F. nucleatum*.

Acknowledgements

This study is funded by the Fundamental Research Grant Scheme (Grant No. FRGS/1/2023/STG01/UITM/02/11) by Ministry of Higher Education and Universiti Teknologi MARA (UiTM) Selangor 42300, Malaysia. Authors acknowledge Atta-ur-Rahman Institute for Natural Product Discovery (AuRIns) and Centre for Medical Laboratory Technology Studies, Faculty of Health Sciences, UiTM Selangor, Malaysia for kindly providing their facilities and resources that supported the completion of this study.

Declaration of Generative AI in Scientific Writing

The authors declare that generative artificial intelligence (AI) tools were employed only to improve language clarity and grammar during manuscript preparation. No aspect of content generation, data interpretation, or scientific analysis involved the use of AI. The authors retain full responsibility for the accuracy and conclusions presented herein.

Credit Author Statement

Nursyamimi Nasuha Suhaimi: Manuscript writing; Experimental work; Data analysis. **Nur Ayunie Zulkepli:** Supervision; Manuscript finalization. **Fatimah Salim:** Supervision; Validation of sample preparation. **Norehan Mokhtar:** Supervision; Validation of biofilm. **Dyaningtyas Dewi Pamungkas Putri:** Manuscript preparation. **Mohd Khairul Ya'kub:** Providing raw samples.

References

[1] AB Lagha, B Haas and D Grenier. Tea polyphenols inhibit the growth and virulence properties of Fusobacterium nucleatum. *Scientific Reports* 2017; **7**, 44815.

[2] YJ Jung, HK Jun and BK Choi. *Porphyromonas gingivalis* suppresses invasion of *Fusobacterium nucleatum* into gingival epithelial cells. *Journal of Oral Microbiology* 2017; **9(1)**, 1320193.

[3] M Hung, R Kelly, A Mohajeri, L Reese, S Badawi, C Frost, T Sevathas and MS Lipsky. Factors associated with periodontitis in younger individuals: A scoping review. *Journal of Clinical Medicine* 2023; **12(20)**, 6442.

[4] X Wen, H Li, S Li, B Chang, S Chen, H Li, C Liu and G Li. Associated factors of periodontitis and predicted study among young man in China: A population-based cross-sectional study. *BMC Public Health* 2024; **24(1)**, 1235.

[5] GBD 2021 Oral Disorders Collaborators. Trends in the global, regional, and national burden of oral conditions from 1990 to 2021: A systematic analysis for the Global Burden of Disease Study 2021. *The Lancet* 2025; **405(10482)**, 897-910.

[6] SM Zayed, MM Aboulwafa, AM Hashem and SE Saleh. Biofilm formation by Streptococcus mutans and its inhibition by green tea extracts. *AMB Express* 2021; **11(1)**, 73.

[7] CJ Henley-Smith, AM Kok, FS Botha, C Baker and N Lall. The effect of a poly-herbal plant extract on the adhesion of Streptococcus mutans to tooth enamel. *BMC Complementary Medicine and Therapies* 2024; **24(1)**, 402.

[8] M Muchova, DL Balacco, MM Grant, ILC Chapple, SA Kuehne and J Hirschfeld. *Fusobacterium nucleatum* subspecies differ in biofilm forming ability *in vitro*. *Frontiers in Oral Health* 2022; **3**, 853618.

[9] M Adnan, AJ Siddiqui, SA Ashraf, MS Ashraf, SO Alomrani, M Alreshidi, B Tepe, M Sachidanandan, C Danciu and M Patel. Saponin-derived silver nanoparticles from *Phoenix dactylifera* (Ajwa Dates) exhibit broad-spectrum bioactivities combating bacterial infections. *Antibiotics* 2023; **12(9)**, 1415.

[10] AMT Lim, GG Oyong, MCS Tan, CC Shen, CY Ragasa and EC Cabrera. Quorum quenching activity of *Andrographis paniculata* (Burm f.) Nees andrographolide compounds on metallo-β-lactamase-producing clinical isolates of *Pseudomonas aeruginosa* PA22 and PA247 and their effect on *lasR* gene expression. *Heliyon* 2021; **7(5)**, 07002.

[11] M Patel, LI Alnajjar, SO Alomrani, N Alshammari, MS Ashraf and M Adnan. *Embelia ribes* Burm.f. fruit extract inhibit quorum sensing-dependent production of virulence factors and biofilm formation: An integrated *in vitro* and *in silico* approach. *South African Journal of Botany* 2024; **165**, 307-323.

[12] K Sauer, P Stoodley, DM Goeres, L Hall-Stoodley, M Burmølle, PS Stewart and T Bjarnsholt. The biofilm life cycle: Expanding the conceptual model of biofilm formation. *Nature Reviews Microbiology* 2022; **20(10)**, 608-620.

[13] P Tritripmongkol, S Sangkanu, R Boripun, J Jeenkeawpieam, J Chuprom, V Nissapatorn, MDL Pereira, AK Paul and W Mitsuwan. Robusta coffee extracts inhibit quorum sensing activity in *Chromobacterium violaceum* and reduce biofilms against *Bacillus cereus* and *Staphylococcus aureus*. *Veterinary World* 2022; **15(10)**, 2391-2398.

[14] Samreen, FA Qais and I Ahmad. Anti-quorum sensing and biofilm inhibitory effect of some medicinal plants against gram-negative bacterial pathogens: *In vitro* and *in silico* investigations. *Heliyon* 2022; **8(10)**, 11113.

[15] M Venkatramanan, PS Ganesh, R Senthil, J Akshay, AV Ravi, K Langeswaran, J Vadivelu, S Nagarajan, K Rajendran and EM Shankar. Inhibition of quorum sensing and biofilm formation in *Chromobacterium violaceum* by fruit extracts of *Passiflora edulis*. *ACS Omega* 2020; **5(40)**, 25605-25616.

[16] CA Santos, FA Almeida, BXV Quecán, PAP Pereira, KMB Gandra, LR Cunha and UM Pinto. Bioactive properties of *Syzygium cumini* (L.) skeels pulp and seed phenolic extracts. *Frontiers in Microbiology* 2020; **11**, 990.

[17] M Molnár, E Fenyvesi, Z Berkl, I Németh, I Fekete-Kertész, R Márton, E Vaszita, E Varga, D Ujj and L Szente. Cyclodextrin-mediated quorum quenching in the *Aliivibrio fischeri* bioluminescence model system - Modulation of bacterial communication. *International Journal of Pharmaceutics* 2021; **594**, 120150.

[18] SJ Khalid, Q Ain, SJ Khan, A Jalil, MF Siddiqui, T Ahmad, M Badshah and F Adnan. Targeting Acyl Homoserine Lactones (AHLs) by the quorum quenching bacterial strains to control biofilm formation in *Pseudomonas aeruginosa*. *Saudi Journal of Biological Sciences* 2022; **29(3)**, 1673-1682.

[19] M Podkowik, AI Perault, G Putzel, A Pountain, J Kim, A Dumont, E Zwack, RJ Ulrich, TK Karagounis, C Zhou, AF Haag, J Shenderovich, GA Wasserman, J Kwon, J Chen, AR Richardson, JN Weiser, CR Nowosad, DS Lun, D Parker, ..., B Shopsin. Quorum-sensing agr system of *Staphylococcus aureus* primes gene expression for protection from lethal oxidative stress. *bioRxiv* 2024. https://doi.org/10.1101/2023.06.08.544038

[20] HY Liu, EL Prentice and MA Webber. Mechanisms of antimicrobial resistance in biofilms. *NPJ Antimicrobials and Resistance* 2024; **2(1)**, 27.

[21] U Kansakar, V Trimarco, MV Manzi, E Cervi, P Mone and G Santulli. Exploring the therapeutic potential of bromelain: Applications, benefits, and mechanisms. *Nutrients* 2024; **16(13)**, 2060.

[22] C Locci, E Chicconi and R Antonucci. Current uses of bromelain in Children: A narrative review. *Children* 2024; **11(3)**, 377.

[23] O Insuan, P Janchai, B Thongchuai, R Chaiwongsa, S Khamchun, S Saoin, W Insuan, P Pothacharoen, W Apiwatanapiwat, A Boondaeng and P Vaithanomsat. Anti-inflammatory effect of pineapple rhizome bromelain through downregulation of the NF-κB- and MAPKs-signaling pathways in lipopolysaccharide (LPS)-stimulated RAW264.7 cells. *Current Issues in Molecular Biology* 2021; **43(1)**, 93-106.

[24] NC Praveen, A Rajesh, M Madan, VR Chaurasia, NV Hiremath and AM Sharma. *In vitro* evaluation of antibacterial efficacy of pineapple extract (bromelain) on periodontal pathogens. *Journal of International Oral Health* 2014; **6(5)**, 96-98.

[25] MP Silva, MA Calomino, LA Teixeira, RR Barros, GR de Paula and FL Teixeira. Antibiofilm activity of bromelain from pineapple against Staphylococcus aureus. *Acta Scientiarum Biological Sciences* 2023; **45(1)**, 65725.

[26] NH Tarmizi, NS Kamarudin, AS Johari, NA Zulkepli, N Mokhtar and MK Ya'Kub. Purification of bromelain enzyme from MD2 hybrid pineapple core by ultrafiltration and its antioxidative potential. *Science, Engineering and Health Studies* 2023; **17**, 23030004.

[27] KY Tsai, PL Wei, M Azarkan, N M'Rabet, PT Makondi, HA Chen, CY Huang and YJ Chang. Cytotoxic properties of unfractionated and fractionated bromelain alone or in combination with chemotherapeutic agents in colorectal cancer cells. *PLoS One* 2023; **18(6)**, 0285970.

[28] PA Hu, SH Wang, CH Chen, BC Guo, JW Huang and TS Lee. New mechanisms of bromelain in alleviating non-alcoholic fatty liver disease-induced deregulation of blood coagulation. *Nutrients* 2022; **14(11)**, 2329.

[29] AS Johari, NH Tarmizi, Y Mk, NA Zulkepli, S Sarmoko and N Mokhtar. *In vitro* antibacterial and antibiofilm activities of ultrafiltrated-bromelain against dental caries pathogens. *Journal of Health and Translational Medicine* 2023; **2**, 233-240.

[30] A Arumugam and V Ponnusami. Pineapple fruit bromelain recovery using recyclable functionalized ordered mesoporous silica synthesized from sugarcane leaf ash. *Brazilian Journal of Chemical Engineering* 2013; **30(3)**, 477-486.

[31] E Millhouse, A Jose, L Sherry, DF Lappin, N Patel, AM Middleton, J Pratten, S Culshaw and G Ramage. Development of an *in vitro* periodontal biofilm model for assessing antimicrobial and host modulatory effects of bioactive molecules. *BMC Oral Health* 2014; **14**, 80.

[32] AA Djais, Jemmy, N Putri, AR Putri and SA Soekanto. Description of *Streptococcus mutans*, *Streptococcus sanguinis*, and *Candida albicans* biofilms after exposure to propolis dentifrice by using OpenCFU method. *Saudi Dental Journal* 2020; **32(3)**, 129-134.

[33] T Roth, E Zelinger, T Kossovsky and G Borkow. Scanning electron microscopy analysis of biofilm-encased bacteria exposed to cuprous oxide-impregnated wound dressings. *Microbiology Research* 2024; **15(4)**, 2358-2368.

[34] RO Adeyemo, IM Famuyide, JP Dzoyem and MGL Joy. Anti-biofilm, antibacterial, and anti-quorum sensing activities of selected south african plants traditionally used to treat diarrhoea. *Evidence-Based Complementary and Alternative Medicine* 2022; **2022**, 1307801.

[35] Y Liu, SG Daniel, HE Kim, H Koo, J Korostoff, F Teles, K Bittinger and G Hwang. Addition of cariogenic pathogens to complex oral microflora drives significant changes in biofilm compositions and functionalities. *Microbiome* 2023; **11(1)**, 123.

[36] DK Fitri, N Tuygunov, WHAW Harun, IA Purwasena, A Cahyanto and MN Zakaria. Key virulence genes associated with *Streptococcus mutans* biofilm formation: A systematic review. *Frontiers in Oral Health* 2025; **6**, 1654428.

[37] Y Chen, T Shi, Y Li, L Huang and D Yin. *Fusobacterium nucleatum*: The opportunistic pathogen of periodontal and peri-implant diseases. *Frontiers Microbiology* 2022; **13**, 860149.

[38] A Luo, F Wang, D Sun, X Liu and B Xin. Formation, development, and cross-species interactions in biofilms. *Frontiers in Microbiology* 2022; **12**, 757327.

[39] H Fu, X Li, R Zhang, J Zhu and X Wang. Global burden of periodontal diseases among the working-age population from 1990-2021: Results

from the Global Burden of Disease Study 2021. *BMC Public Health* 2025; **25(1)**, 1316.

[40] L Rudin, N Roth, J Kneubühler, BN Dubey, MM Bornstein and V Shyp. Inhibitory effect of natural flavone luteolin on *Streptococcus mutans* biofilm formation. *Microbiology Spectrum* 2023; **11(5)**, 0522322.

[41] Y Ham and TJ Kim. Synergistic inhibitory activity of Glycyrrhizae Radix and Rubi Fructus extracts on biofilm formation of Streptococcus mutans. *BMC Complementary Medicine and Therapies* 2023; **23(1)**, 22.

[42] A Fissore, M Marengo, V Santoro, G Grillo, S Oliaro-Bosso, G Cravotto, FD Piaz and S Adinolfi. Extraction and characterization of bromelain from Pineapple core: A strategy for Pineapple waste valorization. *Processes* 2023; **11(7)**, 2064.

[43] FMC Gamarra, JCC Santana, SAV Llanos, JAH Pérez, FR Flausino, APB Quispe, PC Mendoza, RM Vanalle, C Carreño-Farfan, FT Berssaneti, RR de Souza and EB Tambourgi. High retention and purification of bromelain enzyme (*Ananas comosus* L. Merrill) from pineapple juice using plain and hollow polymeric membranes techniques. *Polymers* 2022; **14(2)**, 264.

[44] IRAP Bresolin, ITL Bresolin, E Silveira, EB Tambourgi and PG Mazzola. Isolation and purification of bromelain from waste peel of Pineapple for therapeutic application. *Brazilian Archives of Biology and Technology* 2013; **56(6)**, 971-979.

[45] MZM Nor, L Ramchandran, M Duke and T Vasiljevic. Performance of a two-stage membrane system for bromelain separation from Pineapple waste mixture as impacted by enzymatic pretreatment and diafiltration. *Food Technology and Biotechnology* 2018; **56(2)**, 218-227.

[46] A Sathiaseelan, KP Song, HS Tan and WS Choo. Antibiofilm activity of *Clitoria ternatea* flowers anthocyanin fraction against biofilm-forming oral bacteria. *FEMS Microbiology Letters* 2025; **372**, 035.

[47] A Tada, H Nakayama-Imaohji, H Yamasaki, M Elahi, T Nagao, H Yagi, M Ishikawa, K Shibuya and T Kuwahara. Effect of thymoquinone on Fusobacterium nucleatum-associated biofilm and inflammation. *Molecular Medicine Reports* 2020; **22(2)**, 643-650.

[48] F Moradi, N Hadi and A Bazargani. Evaluation of quorum-sensing inhibitory effects of extracts of three traditional medicine plants with known antibacterial properties. *New Microbes and New Infections* 2020; **38**, 100769.

[49] PD Dimitrova, V Ivanova, A Trendafilova and T Paunova-Krasteva. Anti-biofilm and anti-quorum-sensing activity of *Inula* extracts: A strategy for modulating *Chromobacterium violaceum* virulence factors. *Pharmaceuticals* 2024; **17(5)**, 573.